Erschienen in: Toxicological sciences : an official journal of the Society of Toxicology ; 142 (2014), 1. - S. 274-284

Impairment of Glutamate Signaling in Mouse Central Nervous System Neurons *In Vitro* by Tri-Ortho-Cresyl Phosphate at Noncytotoxic Concentrations

Vanessa Hausherr*,[1], Christoph van Thriel*, Anne Krug†, Marcel Leist†, and Nicole Schöbel*,‡

*IfADo - Leibniz Research Center for Working Environment and Human Factors, 44139 Dortmund, Germany, †Doerenkamp-Zbinden Chair for in vitro toxicology and biomedicine, University of Konstanz, 78462 Konstanz, Germany and ‡Department of Animal Physiology, Ruhr-University Bochum, 44801 Bochum, Germany

[1]To whom correspondence should be addressed at. Leibniz Research Center or Working Environment and Human Factors, Neurotoxicology and Chemosensation, Ardeystr. 67, 44139 Dortmund, Germany. Fax: +49 (0)231-1084-308. E-mail: hausherr@ifado.de.

ABSTRACT

Occupational and environmental exposure to tri-cresyl phosphates (TCPs) may cause various types of neurotoxicity. Among the TCP isomers, tri-ortho-cresyl phosphate is a well-studied organophosphate (OP) known to cause OP-induced delayed neuropathy (OPIDN). Clinically, OPIDN is characterized by limb paralysis caused by the inhibition of neuropathy target esterase. Like other OPs, TOCP may also trigger acute toxicity by yet unknown mechanisms. Neurotoxic effects of TCPs, including TOCP, on central nervous system functions have not been studied in depth, and such non-OPIDN mechanisms might be related to the aerotoxic syndrome. To identify alternative mechanisms of TOCP neurotoxicity, we conducted an *in vitro* study using primary cortical neurons isolated from mouse embryos (E 16.5). After 24 h or 6 days *in vitro* (DIV), cell cultures were treated with different TOCP concentrations for 24 h. On DIV 2 and 7, we investigated three different endpoints—general cytotoxicity, neurite outgrowth, and glutamatergic signaling. At both time points, the EC_{50} for TOCP-induced cell death was 90 μM, however, neurite outgrowth was already significantly affected at TOCP concentrations of 10 μM. The number of cells responding to glutamate, as well as the corresponding mean response amplitudes were reduced with TOCP concentrations as low as 100 nM. For the first time, functional neurotoxicity is observed with very low TOCP concentrations, and in the absence of structural damages. Our proposed mechanism is that TOCP exposure may lead to cognitive deficits relevant in aerotoxic syndrome by inhibiting the signaling of glutamate, the most abundant excitatory neurotransmitter in the brain.

Key words: tri-ortho-cresyl phosphate; neurotoxicity; glutamate signaling; neurite outgrowth inhibition; aerotoxic syndrome

Tri-cresyl phosphate (TCP) exposure, either environmental or occupational, has been associated with neurotoxic outcomes (Abou-Donia, 1993). Among the TCP isomers, the organophosphorus ester tri-ortho-cresyl phosphate (TOCP; CAS 78–30–8) is an important compound used as a plasticizer, plastic softener, flame retardant, and jet oil additive in various industries. International occupational exposure limits have been consistently set to 0.1 mg/m^3 (GESTIS website), and in 1992 the American Conference of Governmental Industrial Hygienists (ACGIH) based their threshold limit value for TOCP on its ability to inhibit acetylcholinesterase (AChE) (ACGIH, 2013). Indeed, TOCP might cause a cholinergic crisis, but its toxicity may be more realistically attributed to organophosphate-induced delayed neuropathy (OPIDN) in the peripheral nervous systems of humans and animals (Abou-Donia, 1993). The clinical signs are based on the inhibition and aging of neuropathy target esterase (NTE) by

TOCP and its metabolite, cresyl saligenin phosphate (CBDP). The affinity of other TCP isomers for AChE and NTE is lower, and as a consequence it was assumed that these compounds are less toxic (Henschler, 1958). In principle, the NTE-related mechanism leads to neuromuscular blockage and muscle weakness resulting in paralysis (Emerick *et al.*, 2010; Eto *et al.*, 1962). However, effects of short-term exposure to TOCP, and the resulting impairment of central nervous system processes can hardly be explained exclusively by effects on NTE. Such neurobehavioral effects have been described recently for another suspected neurotoxic syndrome that might be related to the use of TCPs.

TCPs, including TOCP, that are commonly used as additives in jet gear oil have been proposed as a causative agent of aerotoxic syndrome (AS, see Liyasova *et al.*, 2011) characterized by symptoms and clinical signs associated with acute impairment of central nervous system functions (e.g., difficulties to concentrate). Therefore, the present study was conducted to investigate alternative TOCP modes of action of neurotoxicity that are more likely related to these symptoms.

The nervous system is characterized by the ability to adapt to new challenges by either strengthening or weakening connectivity, a phenomenon also known as neuronal plasticity (Kempermann *et al.*, 2000). These processes are also based on the connectivity between the neurons and the stable neurite network structures. Chemicals are capable of perturbing these processes leading to neurobehavioral effects in animals and humans (van Thriel *et al.*, 2012). Acute exposures to different neurotoxins (e.g., organic solvents, pyrethroids) lead to perturbations of ion channels or receptors initiating and relaying action potentials (Bowen *et al.*, 2006; Cao *et al.*, 2011). Interactions of several organophosphates (OPs), including TOCP, with the glutamatergic N-methyl-D-aspartic acid (NMDA) receptor have been reported previously (Johnson and Michaelis, 1992). Accordingly, the study proposed that TOCP might perturb calcium-dependent membrane depolarization and signaling by changing the ion permeability of ionotropic neurotransmitter receptors (e.g., glutamatergic receptors) or voltage-gated ion channels. Phasic changes in intracellular calcium ions $[Ca^{2+}]_i$ through specialized voltage-gated ion channels in turn are essential for neuronal function. TOCP might affect the $[Ca^{2+}]_i$ by altering the gene expression or function of ligand-gated or voltage-gated ion channels.

Together, current knowledge about alternative OP neurotoxicity and pathways of neurotoxicity in general (Bushnell *et al.*, 2010) suggest that TOCP might impair the functionality of central nervous system neurons. Until now, this possible effect of TOCP exposure has not been addressed using *in vitro* or *in vivo* models. Therefore, the present study aimed at characterizing the neurotoxic effects of TOCP in primary neurons isolated from the mouse central nervous system by assessing different endpoints. Cell viability was investigated as a general parameter of toxicity; whereas, neurite outgrowth was measured as a specific parameter of neurotoxicity (Harrill *et al.*, 2011). Furthermore, neurochemical processes were analyzed as an endpoint of functional neurotoxicity, using fluorescence-based live-cell calcium imaging. We here tested the TOCP effects on signals evoked by the excitatory neurotransmitter glutamate, and the resulting effects on voltage-gated calcium channels. The selection of the three different endpoints was motivated by the expectation of an unequivocal concentration-dependency. We hypothesized a reduction in neuronal viability and structure at high TOCP concentrations, and altered postsynaptic signaling at comparably low concentrations.

MATERIALS AND METHODS

Animals. All experiments involving animals were performed in accordance with the European Union Community Council guidelines and all measures were taken to reduce animal suffering to a minimum. CD1 mice (Charles River Laboratories, Sulzfeld, Germany) were housed in standard cages with standard laboratory chow and drinking water *ad libitum*.

Preparation and cell culture. Primary cortical neurons (pCNs) of mice were isolated as described previously (Dinh *et al.*, 2013) with minor changes. Briefly, cortical neurons were isolated from CD1 mouse embryos at embryonic day 16.5. After anesthetization with CO_2, dams were sacrificed by cervical dislocation. Their abdomina were opened and embryos were dissected from uterine tissue. After quick decapitation, the embryo's skull was opened, the brain removed, and transferred into ice-cold HBSS (Hanks Balanced Salt Solution, 5.3 mM KCl, 0.44 mM KH_2PO_4, 4.16 mM $NaHCO_3$, 137.93 mM NaCl, 0.33 mM Na_2HPO_4, 5.55 mM D-glucose, and 0.026 mM phenol red). Hemispheres were separated, the meninges removed, and the segregated cortices were transferred to fresh ice-cold HBSS. After washing, cortices were trypsinized for 10 min at 37°C. The trypsin reaction was stopped by soybean trypsin inhibitor (0.25 mg/ml) and 0.01% (v/v) DNase. Cortices were then triturated, followed by centrifugation for 5 min at 1000 rpm. The cell pellet was resuspended in neurobasal media supplemented with 2% (v/v) B27, 0.5 mM stable glutaminem, and 0.1% (v/v) gentamycin. Cells were seeded on poly-L-lysine (PLL)-coated glass cover slips (Ø = 14 mm, Menzel) or plastic surfaces at a density of 40,000 cells/cm^2 and cultured at 37°C in a humidified atmosphere containing 5% CO_2. By using this particular protocol the cell culture consisted of approximately 95% neurons since the growth and proliferation of glial cells was suppressed. In agreement with their cortical origin nearly 100% of the cells responded to glutamate. For each data set of the different readouts (e.g., cell viability), cells from 3 to 5 independent biological replicates were investigated. Before treatment with TOCP for 24 h the pCNs were kept in cell culture for 24 h or 6 days. Accordingly, the various readouts were collected either on days *in vitro* (DIV) 2 or DIV 7. TOCP was dissolved and diluted in dimethyl sulfoxide (DMSO) and used from stock solution at 1:1000 diluted in medium. The maximal DMSO concentration was 0.1 % in media. In addition, 0.1% DMSO was used as solvent control.

Chemicals. TOCP (>96%) was purchased from TCI Chemicals (Eschborn, Germany). Neurobasal media, B27 supplement, gentamycin, HBSS, phosphate buffered saline (PBS), 4′, 6-diamidino-2-phenylindole (DAPI), and soybean trypsin inhibitor were purchased from Gibco (Darmstadt, Germany). Stabilized glutamine and trypsin were purchased from PAN-biotech (Aidenbach, Germany). PLL and Deoxyribonuclease I from bovine pancreas (DNase) were purchased from Sigma Aldrich (Hamburg, Germany). Polyclonal mouse anti-β-III-tubulin (MMS-435P) and polyclonal rabbit anti-β-III-tubulin (PRB-435P) were purchased from HISS (Freiburg, Germany). Normal donkey serum, donkey anti-mouse Dylight649, and donkey anti-rabbit Dylight488 antibodies were purchased from Dianova (Hamburg, Germany). Fluor Preserve™ Reagent was purchased from Calbiochem (Darmstadt, Germany). Triton X-100 was purchased from Roth (Karlsruhe, Germany). Fura-2/AM was purchased from Tocris (Bristol, United Kingdom). CTB Assay Kit was purchased from Promega (Mannheim, Germany).

CellTiter Blue cell viability assay. Cell viability was determined by the fluorimetric, resazurin-based CellTiter Blue (CTB) assay in black 96-well plates (Greiner bio, Frickenhausen, Germany) according to the manufacturer's instructions. In brief, cells were seeded at a density of 12,000 cells per well and grown for 24 h or 6 DIV. Cells were then treated with different concentrations of TOCP for 20 h, followed by 4 h incubation with CTB reagent. The fluorescence was measured at 540/595 nm with the Tecan infinite M200 Pro plate-reader. Cell viability was calculated and expressed as a percentage of control.

Immunocytochemistry. Mouse cortical neurons were treated with TOCP for 24 h, washed twice with PBS, fixed with 4% (v/v) paraformaldehyde for 15 min, and cell membranes were permeabilized with 0.1% (v/v) Triton X-100 in PBS for 10 min. Nonspecific binding sites were blocked using 5% (v/v) normal donkey serum in PBS for 1 h. Cells were incubated with polyclonal mouse anti-β-III-tubulin diluted 1:500 for 2 h at room temperature, followed by incubation with donkey anti-mouse Dylight649 (1:500) for 30 min. Nuclei were stained with DAPI (4′, 6-diamidino-2-phenylindole) diluted 1:10,000 for 30 min. Cover slips were mounted on microscopic glass slides with Fluor Preserve™ Reagent. Images were analyzed with the Leica DMI 6000 B microscope, the monochrome CCD camera DFC 360 FX, and the Leica LAS AF 600 Software (version 2.6.0.7266).

Quantitative analysis of neurite area — high-throughput method. Cells were treated with different TOCP concentrations and incubated for 24 h under standard cell culture conditions. Cells were stained as described above with polyclonal rabbit anti-tubulin and donkey anti-rabbit DyLight488 and DAPI. Neurite area was measured as previously described in Stiegler *et al.* (2011) and Krug *et al.* (2013). In brief, the cell culture plates were loaded into an automated microplate-reading microscope (Array-Scan VI HCS Reader, Cellomics) with a Hamamatsu OCRA-ER camera. For each well, 10 randomly selected fields of view were scanned in two channels (10-fold objective, 2 × 2 pixel binning). In channel 1, DAPI was detected with an excitation/emission wavelength of 365 ± 50 nm/535 ± 54 nm to identify nuclei based on size, area, shape, and intensity, whereas β-III-tubulin was detected with an excitation/emission wavelength of 474 ± 40 nm/535 ± 45 nM in channel 2. The nuclear outlines were expanded in each direction to define a virtual cell soma area (VCSA). All β-III-tubulin-positive pixels of the field were defined as neuronal cellular structures (NCSs). In an automatic calculation, the VCSAs were used as a filter in the β-III-tubulin channel and subtracted from the NCS. The remaining pixels (NCS – VCSA) in the β-III-tubulin channel were defined as neurite area.

Quantitative analysis of neurite outgrowth — IMARIS. IMARIS software (Bitplane, Zurich, Switzerland) was used to analyze details of neurite morphology. Based on fluorescence images of the TOCP-treated and control neurons (β-III-Tubulin and DAPI staining), a reconstruction of neuronal structures was conducted. After reconstruction, the IMARIS software enables the quantification of neurite length and neurite diameter.

Calcium imaging. Calcium imaging studies were performed as described previously (Schöbel *et al.*, 2012) with minor changes. In brief, cortical neurons were incubated with 3 mM Fura-2/AM at 37°C and 5% CO_2 for 35 min. Glass slides were transferred into inherent polytetrafluoroethylene measuring chambers filled with standard extracellular buffer (140 mM NaCl, 5 mM KCl, 2 mM $CaCl_2$, 1 mM $MgCl_2$, 10 mM HEPES, pH 7.4 (NaOH/HCl), 310 mOsmol (glucose)) that were mounted on a Leica DMI 6000 B microscope equipped with a 20-fold fluorescence-optimized objective (Leica). Cells were exited intermittently at wavelengths of 340 nm (80 ms) and 380 nm (20 ms). Emitted light of 510 nM was detected with the monochrome charge-coupled device (CCD) camera DFC 360 FX. Imaging data were analyzed with the Leica LAS AF 600 Software (version 2.6.0.7266). Changes in intracellular calcium levels were measured as the ratio of emitted light intensity (510 nM) resulting from illumination at 340 and 380 nm (f_{340}/f_{380}). For stimulus application, a hydrostatic pressure-driven 8-in-1 application system was used. The application cannula was placed in close proximity of the cells to enable precise substance application. At the end of every experiment, neurons were stimulated with a short (5 s) pulse of depolarizing extracellular buffer containing 45 mM KCl (100 mM NaCl, 45 mM KCl, 2 mM $CaCl_2$, 1 mM $MgCl_2$, 10 mM HEPES, pH 7.4 (NaOH/HCl) 310 mOsmol). Time series of the imaging data were exported as Microsoft™ Excel™ compatible files, and responses and their respective amplitudes were calculated from baseline using Excel macros. A threshold criterion of "amplitude plus four times standard deviation (4 sigma)" was used to detect such responses from the unspecific fluctuation of the f_{340}/f_{380} values (baseline variation). The percentage of glutamate responders and percentage of KCl-responsive neurons are given as responders among all identified cells in the view field. Based on the ratio ΔR (f_{340}/f_{380}) at the beginning of the measurement (10 s) the basal calcium level was calculated. For each cell, baseline calcium levels were calculated as the average of 10 consecutive time points.

Quantitative real-time PCR. RNA isolation of primary cultures of mouse cortex neurons was performed using the innuPREP mini kit (Analytikjena, Jena, Germany) following manufacturer instructions. Reverse transcriptase PCR was performed with iScript cDNA Synthesis Kit (Bio-Rad, Munich, Germany). TaqMan probes Mn00433820_m1 for *grin2b* (NMDA subunit) and Mn22433753_m1 for *gria1* (α-amino-3-hydroxy-5-methy-4-isoxazolepropionic acid receptor (AMPA) subunit, Applied Bio systems, Darmstadt, Germany) were used as fluorescence-monitoring system for DNA amplification. The expression of *gapdh* (glyceraldehyde-3-phosphate dehydrogenase) was used as an endogenous control to standardize the samples. The quantitative real-time PCR was performed in duplicate with the ABI 7500 Fast Real-Time PCR system from Applied Bio systems. Relative quantification was calculated by using the comparative threshold $\Delta\Delta C_T$ — method described previously (Schmittgen and Livak, 2008).

Statistical analysis. All statistical analyses were performed using SPSS Version 21 (IBM Corp.). General (GLM) or generalized linear models (GENLIN) were used to analyze the effect of the applied concentrations and stability of possible effects across the biological replicates. The concentration was treated as fixed effect while the biological replicates (3–5 repetitions) were treated as random effects. According to the levels of measurement, *F* or Wald Chi^2 values were used to determine the significance of the treatment effect. To account for different variances in the different treatment groups Dunnett-T3 post hoc tests were used to compare the respective control condition with the various TOCP concentrations. Pairwise comparisons to the control condition using the Wald-type 95% confidence interval were used to identify significant differences for the number of responders (binary variable). For the analysis of the IMARIS parameter, multivariate tests of both parameters were performed to evaluate the over-

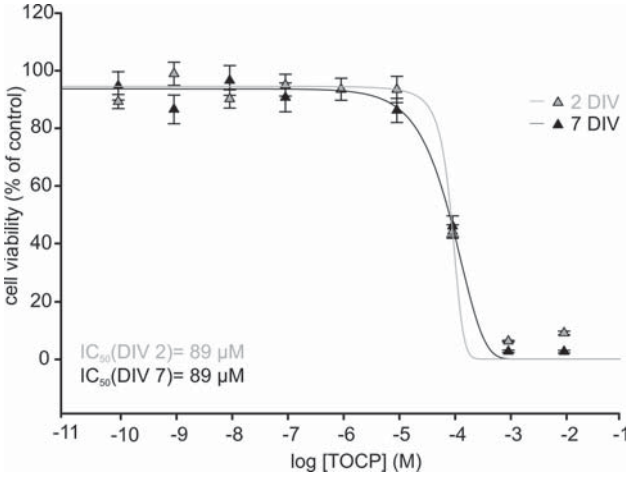

FIG. 1. Effects of TOCP on cell viability. Identification of the cytotoxic and non-cytotoxic concentration range of TOCP. Cell viability of mouse pCNs after 24 h TOCP treatment on DIV 2 and DIV 7 were determined by CTB assay. Concentration response curves were fitted and EC_{50} was calculated. Data are mean ± SEM of three independent biological experiments.

all effect. Subsequently, univariate tests and post hoc tests were applied. Statistical significance was set at $p < 0.05$ and multiple comparisons were adjusted by Bonferroni correction.

RESULTS

TOCP Impairs Cell Viability at High Concentrations

As a first step toward elucidating the neurotoxicity of TOCP in primary cultures of cortex neurons (pCNs), we tested its general cytotoxicity using resazurin-reduction assays. Mouse pCNs were treated with nine TOCP concentrations ranging from 100 pM to 10 mM as well as with 0.1% (v/v) DMSO as the corresponding solvent control. Cells were always incubated for a fixed time period of 24 h beginning at 24 h or 6 days *in vitro*. Cell viability was assessed as percent of control and plotted against the concentration (Fig. 1). There was a concentration-dependent decrease in cell viability in samples treated with millimolar and high micromolar concentrations. At 1 mM TOCP, no viable cells were detectable (see Supplementary fig. 1). No effect on cell viability was observed in cells exposed to 1 µM TOCP and lower concentrations. For DIV 2 and DIV 7 the half-maximal inhibiting concentration (IC_{50}) of cell viability was 89 µM (95% CI (DIV 2): 84–96 µM; 95% CI (DIV 7): 86–101 µM).

TOCP Inhibits Neurite Outgrowth and Induces Neurite Degeneration

At 24 h or 6 days *in vitro*, mouse pCNs were treated with TOCP concentrations of 10 µM, 1 µM, 100 nM, 10 nM, 1 nM, and 0.1% DMSO as the solvent control for 24 h. The neurite area of immunostained cells was analyzed on DIV 2 and DIV 7 by using an automated microplate-reading microscope (Fig. 2A and B). On DIV 2 neuronal cultures treated with TOCP showed a significant reduction in neurite area ($F = 12.75$, $p < 0.001$). Post hoc comparisons revealed that treatment with 1 µM TOCP reduced the neurite area by 40% from 66,000 ± 4000 pixels in the control condition to 40,000 ± 3000 pixels. Applying 10 µM TOCP decreased the neurite area by 60% to 26,000 ± 2000 pixels. On DIV 7, treatment with TOCP significantly reduced the neurite area ($F = 22.94$, $p < 0.001$). Figure 2B shows that compared to the control condition TOCP concentrations of 1 and 10 µM significantly reduced the neurite area (Control: 387,000 ± 31,000 pixels, 1 µM TOCP:

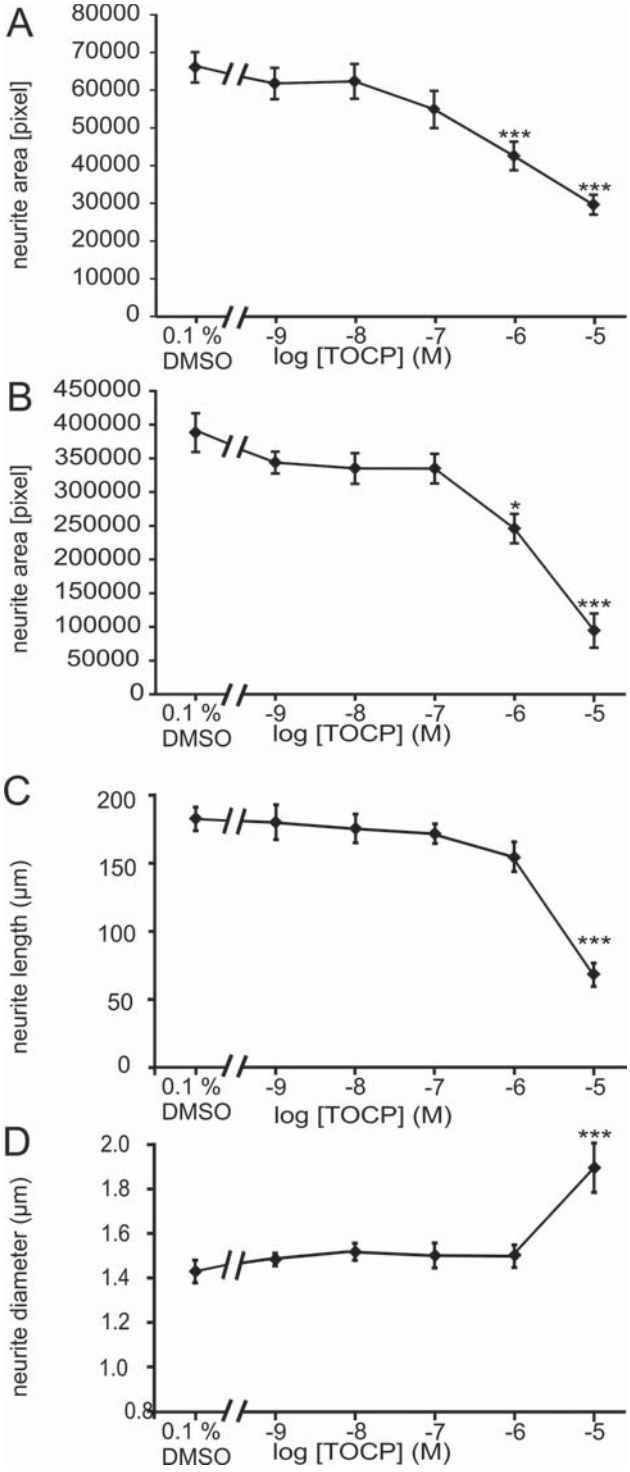

FIG. 2. Quantitative analysis of neurite area and neurite outgrowth parameters of pCNs. TOCP-induced reduction of the neurite area after 24 h treatment on DIV 2 (A) and DIV 7 (B). TOCP induced reduction of neurite length (C) and increase of the neurite diameter (D) on DIV 2. Bars in (A)–(D) show means ± SEM of three independent biological replicates. Results of Dunnett-T3 post hoc tests are indicated as $^{*}p < 0.05$; $^{**}p < 0.01$; $^{***}p < 0.001$.

233,000 ± 28,000 pixels (reduction: 40%) and 10 μM TOCP: 70,000 ± 6,000 pixels (reduction: 82%)). Interestingly, neurite area was reduced at TOCP concentrations that did not trigger general cytotoxicity.

On DIV 2, neurite length (Fig. 2C) and neurite diameter (Fig. 2D) were calculated by using IMARIS software tool. Alterations of both parameters revealed that the neuritic structures were reduced by TOCP ($F = 2.97$, $p < 0.001$). Treatment with 10 μM TOCP had significant effects on neurite length and neurite diameter. The average total neurite length per neuron decreased by more than 60% from 182 ± 8 μm in the control to 68 ± 9 μm after treatment with 10 μM TOCP. Concurrently, neurite diameter increased from 1.4 ± 0.05 μm in the control to 1.9 ± 0.1 μM after 10 μM TOCP treatment.

TOCP Impairs Glutamate Sensitivity

As a next step toward elucidating the possible effects of TOCP on parameters of glutamate signaling and depolarization, we determined the EC_{50} of glutamate for calcium influx in our cell system. Thus, pCNs were stimulated with randomized concentrations of glutamate during live-cell calcium imaging measurement, yielding an EC_{50} value of 33 ± 1.3 μM (95% CI: 31.5–34.5 μM) (see Supplementary fig. 2) with respect to mean amplitudes. After having identified the half-maximally activating glutamate concentration, we stimulated mouse pCNs with 30 μM glutamate for 5 s, after 24 h preincubation with TOCP. Exemplary traces of glutamate-induced responses of these pretreated cells are shown in Figure 3A for DIV 2 and in Figure 4A for DIV 7. Furthermore, the responsiveness to buffer containing 45 mM KCl was evaluated as a measure of the general functionality of neuronal cells in response to a depolarizing stimulus. The percentage of glutamate-responsive neurons (Fig. 3B), the percentage of KCl-responsive cells (Fig. 3C), the glutamate-induced mean response amplitudes (Fig. 3D), the KCl-induced mean response amplitudes (Fig. 3E), and the basal calcium levels (Fig. 3F) for DIV 2 were calculated and are shown in Figure 3. Response frequencies and amplitudes seen upon glutamate as well as KCl stimulation were altered in a concentration-dependent manner by TOCP preincubation. On DIV 2, a significantly smaller fraction of pCNs treated with TOCP concentrations ≥1 nM displayed calcium responses upon glutamate stimulation (i.e., glutamate responders) in comparison to controls (Wald Chi^2: 26.03; $p < 0.001$). More precisely, 61 ± 4% of control cells responded to glutamate; whereas, 1 nM TOCP treatment reduced the number of responding cells to 46 ± 4% and treatment with 10 nM TOCP to 45 ± 4%. TOCP treatment with 100 nM reduced the percentage of glutamate responders to 40 ± 4%, whereas 1 μM TOCP reduced the percentage of responding cells to 36 ± 4%. Following 10 μM TOCP treatment, only 4 ± 2% of the cells responded to glutamate. The mean glutamate-induced response amplitudes were also significantly affected by all tested TOCP concentrations ($F = 20.1$; $p < 0.001$). Neurons treated with TOCP concentrations of 1 nM and higher showed lower mean response amplitudes in comparison to controls. Control cells displayed a mean response amplitude of ΔR (f_{340}/f_{380}) = 0.08 ± 0.0085. TOCP treatment with 1 nM for 24 h reduced the amplitudes to 0.056 ± 0.0069 (70% of control), 10 mM TOCP to 0.038 ± 0.0045 (47% of control), 100 nM to 0.038 ± 0.0049 (47% of control), while 1 μM TOCP reduced the amplitude to ΔR (f_{340}/f_{380}) = 0.032 ± 0.0044 (40% of control). After 10 μM TOCP treatment, responses to glutamate were almost completely abolished (ΔR (f_{340}/f_{380}) = 0.0032 ± 0.0012 (4% of control)). Significant decreases in response frequencies (Wald Chi2: 50.18; $p < 0.001$) to KCl buffer were seen after preincubation with TOCP concentrations ≥10 nM in comparison to controls (0 ± 0% (10 μM TOCP), 67 ± 4% (1 μM TOCP), 76 ± 3% (100 nM TOCP), 84 ± 3% (10 nM TOCP) vs. 95 ± 2% (control)). The corresponding mean response amplitude ($F = 16.29$; $p < 0.001$) induced by KCl buffer was reduced after preincubation with 1 and 10 μM TOCP in comparison to controls (control: ΔR (f_{340}/f_{380}) = 0.109 ± 0.0055, 1 μM: ΔR (f_{340}/f_{380}) = 0.06 ± 0.0054 (55% of control), 10 μM TOCP: ΔR (f_{340}/f_{380}) = 0.0 ± 0.0 (0% of control). At lower concentrations, no such effects were observed. The basal calcium level was increased by 60% at 10 μM TOCP (Fig. 3F).

The general responsiveness of mouse pCNs to glutamate increased over the course of cultivation. In the control conditions, the percentage of glutamate responders increased from 61 ± 4% on DIV 2 to 94 ± 2% on DIV 7. The glutamate-induced mean response amplitude increased from ΔR (f_{340}/f_{380}) = 0.08 ± 0.0085 (DIV 2) to ΔR (f_{340}/f_{380}) = 0.139 ± 0.0089 (DIV 7). The percentage of KCl responders increased from 95 ± 2% to 99 ± 1% and the corresponding mean response amplitude from ΔR (f_{340}/f_{380}) = 0.109 ± 0.0055 to ΔR (f_{340}/f_{380}) = 0.146 ± 0.0066.

Primary cortical neurons treated with TOCP after DIV 7 also showed reduced sensitivity to glutamate stimulation. Figure 4 displays the percentage of glutamate and KCl responders (Fig. 4B and C), the mean glutamate and KCl-induced response amplitudes (Fig. 4D and E), and the basal calcium levels of TOCP-treated cells (Fig. 4F). Again, the percentage of glutamate responders was significantly affected by the TOCP treatment (Wald Chi^2: 25.75; $p < 0.001$). A reduction was seen after treatment with TOCP concentrations of 100 nM–10 μM, control: 94 ± 2% versus 100 nM: 65 ± 3% versus 1 μM: 65 ± 3% versus 10 μM: 23 ± 3%. The mean response amplitudes decreased ($F = 39.26$; $p < 0.001$) after preincubation with TOCP concentrations ≥100 nM (control: ΔR (f_{340}/f_{380}) = 0.139 ± 0.0089 vs. 100 nM: ΔR (f_{340}/f_{380}) = 0.086 ± 0.008 (57% of control) vs. 1 μM: ΔR (f_{340}/f_{380}) = 0.053 ± 0.005 (35% of control) vs. 10 μM: ΔR (f_{340}/f_{380}) = 0.016 ± 0.0026 (11% of control)). A significant decrease in the percentage of responding cells (Wald Chi^2: 3.74; $p < 0.59$) and the amplitudes ($F = 25.17$; $p < 0.001$) after KCl stimuli was observed for 10 μM TOCP. No effects were observed at lower concentrations: (controls: 99 ± 1% of cells, ΔR (f_{340}/f_{380}) = 0.146 ± 0.0066), 10 μM TOCP: 33 ± 3%, ΔR (f_{340}/f_{380}) = 0.042 ± 0.0055 (28% of control)). The basal calcium level was increased at 10 μM TOCP.

TOCP Impairs Glutamate Receptor Expression

To obtain initial hints concerning the underlying mechanisms of the reduced glutamate sensitivity after TOCP preincubation, we tested the expression levels of two glutamate receptor subunits by qRT-PCR. We chose *gria1* (AMPA receptor subunit) and *grin2b* (NMDA receptor subunit) for our analysis. Mouse pCNs were treated with TOCP concentrations between 10 nM and 10 μM as well as 0.1% DMSO (v/v) as a solvent control for 24 h. Cell treatment started at 24 h or 6 days *in vitro*. The expression of *gapdh* was not affected by any of the tested TOCP concentrations on either day — DIV 2 ($F = 0.3$; $p = 0.88$) and DIV 7 ($F = 0.5$; $p = 0.69$). The expression levels of *gria1* (Fig. 5A and C) and *grin2b* (Fig. 5B and D) were calculated for DIV 2 and DIV 7. On DIV 2, a significant decrease in the expression levels of both *gria1* ($F = 9.7$; $p < 0.001$) and *grin2b* ($F = 8.13$; $p < 0.01$) were observed with 10 μM TOCP. On DIV 7, the NMDA receptor subunit expression ($F = 0.59$; $p = 0.67$) and the AMPA receptor subunit expression ($F = 1.85$; $p = 0.13$) was reduced, but the observed alterations were not significant.

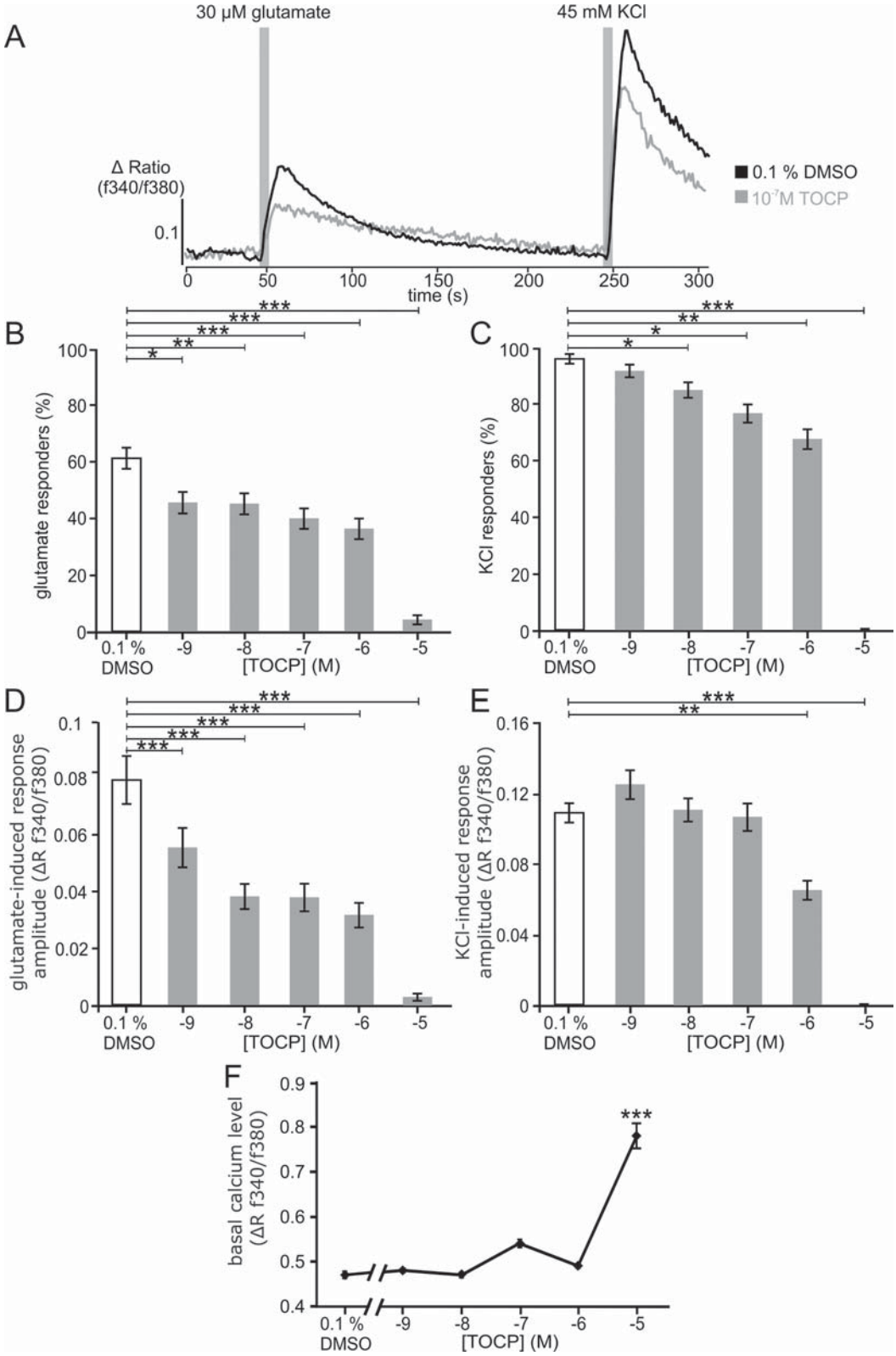

FIG. 3. TOCP impairs glutamate and KCl induced Ca^{2+}-responses of mouse pCNs on DIV 2. $[Ca^{2+}]$ was measured by fura-2AM fluorometry. Exemplary trace of glutamate and KCl induced Ca^{2+}-responses (A) for 0.1% DMSO as solvent control and TOCP treated cells. Percentage of glutamate responders (B) and glutamate-induced response amplitudes (D, amplitudes of nonresponders was set to zero) after 24 h treatment with various TOCP concentrations and 0.1% DMSO as a solvent control. Percentage of KCl responders (C) and KCl-induced response amplitudes (E, amplitudes of nonresponders was set to zero) of pCNs after 24 h treatment with various TOCP concentrations and 0.1% DMSO as control. (F) Steady-state calcium levels are shown after 24 h continued treatment with TOCP at various concentrations. Bars in (B)–(F) show mean ± SEM. Results of Dunnett-T3 post hoc tests are indicted as $^{*}p < 0.05$; $^{**}p < 0.01$; $^{***}p < 0.001$.

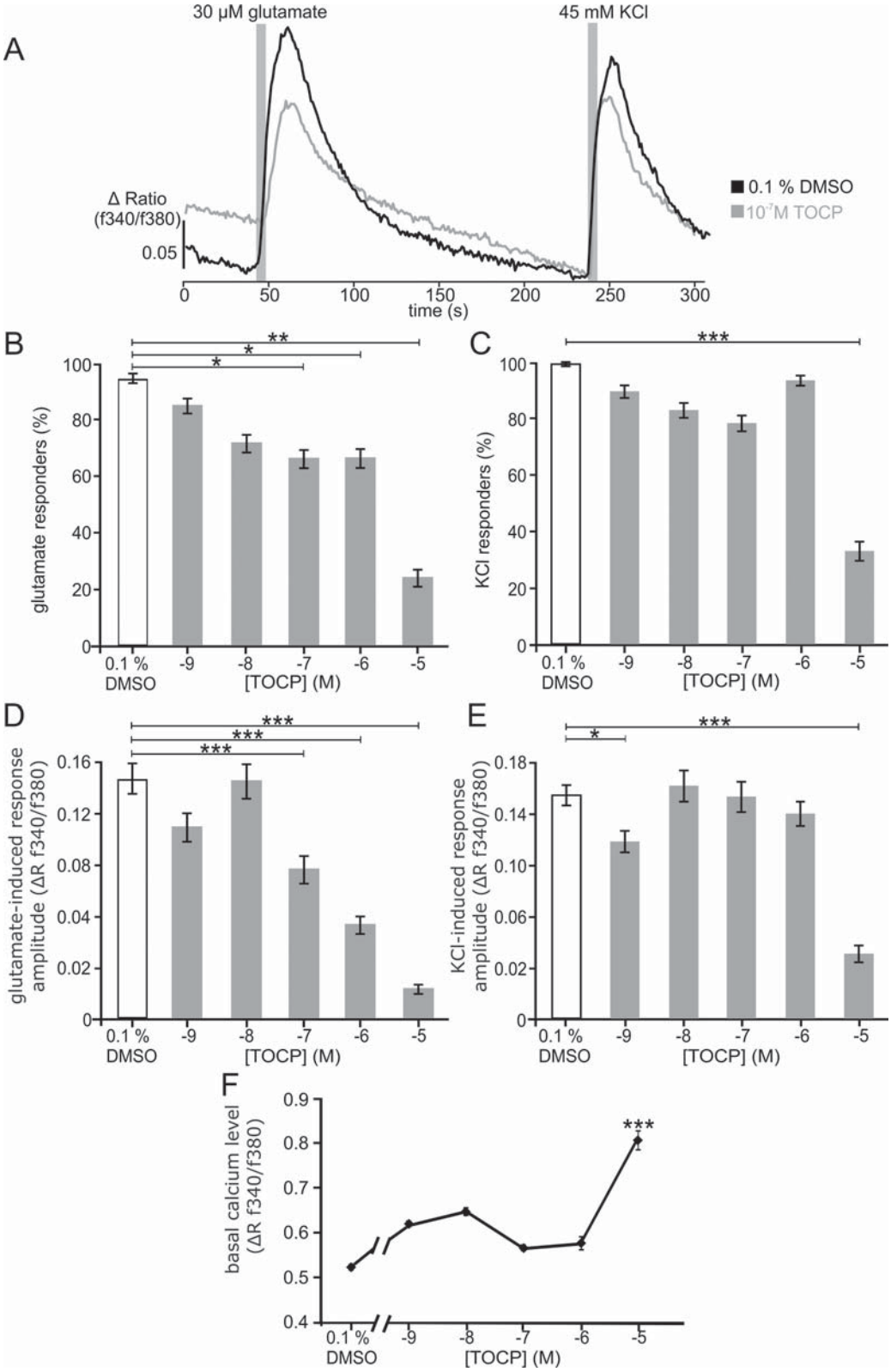

FIG. 4. TOCP impairs glutamate and KCl-induced Ca^{2+}-responses of mouse pCNs on DIV 7. $[Ca^{2+}]$ was measured by fura-2AM fluorometry. Exemplary trace of glutamate and KCl induced Ca^{2+}-responses (A) for 0.1% DMSO as a solvent control and TOCP treated cells. Glutamate responders (B) and glutamate-induced response amplitudes (D, amplitudes of nonresponders was set to zero) of pCNs after 24 h treatment with various TOCP concentrations and 0.1% DMSO as a control. Percentage of KCl responders (C) and KCl-induced response amplitudes (E, amplitudes of nonresponders was set to zero) of mouse pCNs after 24 h treatment with various TOCP concentrations and 0.1% DMSO as a control. (F) Steady-state calcium levels are shown after 24 h continued treatment with TOCP at various concentrations. Bars in (B)–(E) show mean ± SEM. Results of Dunnett-T3 post hoc tests are indicted as $^{*}p < 0.05$; $^{**}p < 0.01$; $^{***}p < 0.001$.

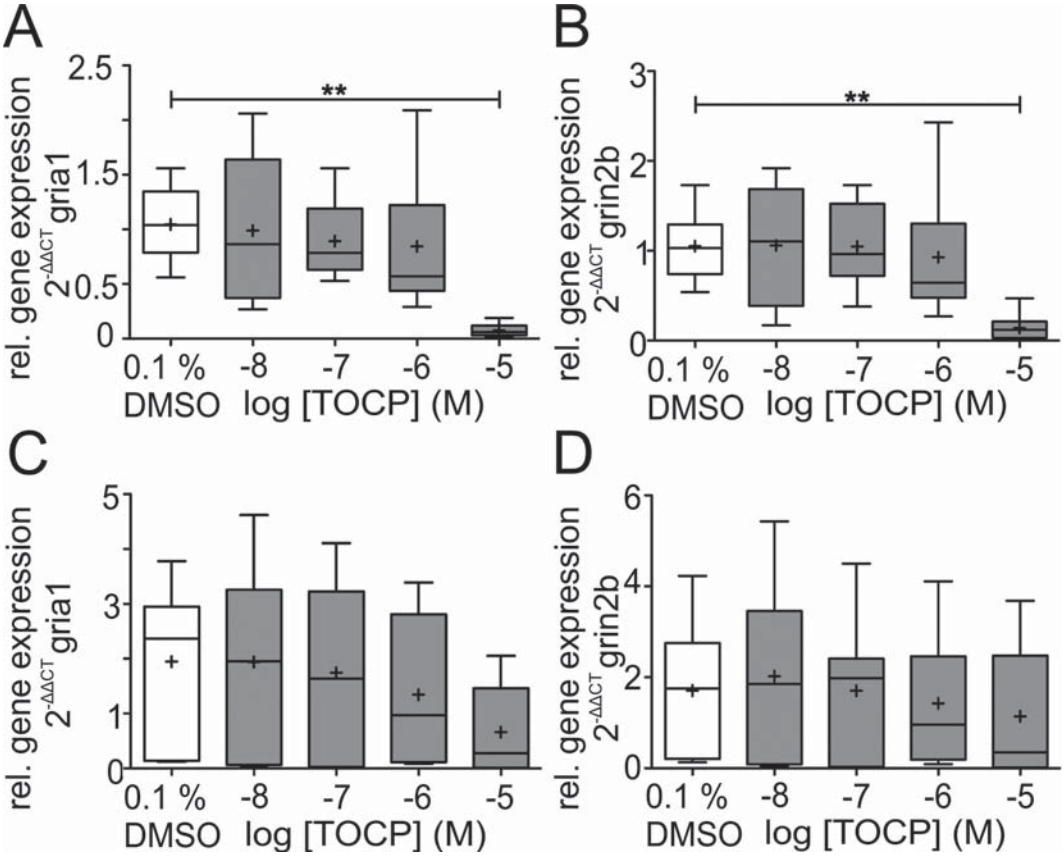

FIG. 5. Influence of TOCP on AMPA receptor subunit *gria1* (A and C) and NMDA receptor subunit *grin2b* (B and D) expression on DIV 2 and 7. PCNs were treated at both time points with various TOCP concentrations for 24 h and expression levels were analyzed. Receptor expression decreased concentration-dependently. Bars in (A)–(D) show mean ± SEM of three independent biological replicates. Results of Dunnett-T3 post hoc tests are indicted as $^{*}p < 0.05$; $^{**}p < 0.01$; $^{***}p < 0.001$.

DISCUSSION

In the present study, we found that TOCP treatment affected functional aspects of mouse pCNs at nanomolar to micromolar concentrations. In accordance with our hypothesis, the different readouts of functional and structural neurotoxicity were differentially affected depending on the concentration of TOCP used.

In comparison with previous *in vitro* studies, primary cells seem to be particularly sensitive to the neurotoxic effects of TOCP. Regarding cytotoxic effects, Chen *et al.* (2013) showed that the viability of SH-SY5Y cells was not affected after 24 h incubation with concentrations of TOCP ranging from 200 μM to 1 mM. Chang and Wu, (2006) showed that in SK-N-SH cells, cell viability was reduced by 50% after treatment with 5 mM TOCP for 12 h. In contrast, we found that TOCP reduced the viability of pCNs to 50% at a concentration of 89 μM, indicating a higher susceptibility of primary neurons in comparison to neuroblastoma cell lines.

OPs are not only cytotoxic to neurons and neuronal cell lines; they also have more subtle effects such as altering neurite morphology and outgrowth. Neurites, as interconnecting structures between neurons and the initial process of neurite outgrowth serve as specific readout for *in vitro* neurotoxicity testing and developmental testing (Frimat *et al.*, 2010; Harrill *et al.*, 2011; Krug *et al.*, 2013). TOCP affected neurite structures in differentiated N2a and PC12 cells as well as in retinoic acid-differentiated SH-SY5Y cells at concentrations of 200 μM to 1 mM (Chen *et al.*, 2013; Flaskos, 2012; Flaskos *et al.*, 1998). The present study shows that TOCP also affected neurite structures in pCNs of mice in a concentration-dependent manner at two different time points. The estimation of neurite areas, quantified by the automated microplate-reading system, showed a reduction in area on DIV 2 and DIV 7 when pretreated with 1 and 10 μM of TOCP, respectively. On DIV 2, the neurite area was almost six times lower than on DIV 7 indicating a less dense network of neurites. This different neurite density and the lower TOCP concentration that generated an effect on DIV 2 suggest that early stages of network formation seem to be more sensitive to TOCP effects.

We investigated neurite structures using the IMARIS software, which facilitates the detailed analysis these neuron-specific patterns. The reconstruction seems to be less sensitive than calculation of neurite area. Using the microplate system, we were able to identify effects for TOCP at 1 μM that were not detectable with IMARIS. On DIV 2, neurite length as well as neurite diameter, as a parameter of axon swelling, were calculated. TOCP is known to induce axon swelling *in vivo* as an early pathological event in OPIDN (Abou-Donia *et al.*, 1988). As confirmation, we found a TOCP-induced increase in neurite diameter in pCNs with 10 μM. Possible mechanisms of *in vivo* and *in vitro* axon swelling and neurite degeneration, suggested in various studies (Chang and Wu, 2006; Song *et al.*, 2009; Song *et al.*, 2012), include the aggregation and deprivation of neurofilaments, β-III-tubulin, and microtubule-associated proteins. Recently, another mechanism involved in the degeneration of cytoskeletal proteins and neurite outgrowth inhibition, namely, the self-degradation process of autophagy has been described (Chen *et al.*, 2013). TOCP induced autophagy in differentiated

SH-SY5Y cells, based on increased levels of autophagy protein LC3-II and an altered LC3-II/LC3-ratio. These recent findings on the molecular mechanisms underlying TOCP's neurotoxic effect should be included in further studies. In summary, the mouse pCNs that we used in our experiments displayed a higher sensitivity toward TOCP-induced neurite outgrowth inhibition than the cell lines used in previous studies.

OPs influence different neurotransmitter systems, for instance the dopaminergic and cholinergic systems (Pung *et al.*, 2006), as well as the neurotransmitters serotonin (Slotkin *et al.*, 2008), glutamate, and GABA (Gant *et al.*, 1987). Glutamate is the main excitatory neurotransmitter in the brain and is involved in various central nervous system functions, like cognition, memory, and learning (Danbolt, 2001). In the present study, we could for the first time show that even low concentrations of TOCP that do not affect cell viability or neurite structures, impair glutamate-induced signals in pCNs after a relatively short exposure time of 24 h. On DIV 2, the percentage of glutamate responders and the corresponding mean response amplitudes were reduced after treatment with 1 nM TOCP. On DIV 7, the percentage of glutamate responders in addition to the glutamate-induced response amplitudes were reduced with 100 nM TOCP. On DIV 2, the KCl-induced amplitudes as well as the percentage of responding cells were reduced after treatment with concentrations between 10 nM and 10 μM TOCP. Conversely, on DIV 7 only 10 μM TOCP treatment significantly reduced the percentage of KCl responders as well as the corresponding mean response amplitude. Interestingly, KCl-induced responses were affected at much higher concentrations than those to glutamate. It, therefore, appears that TOCP does not affect general neuronal processes at very low concentrations, but rather specifically impairs glutamate signaling. Treatment with 10 μM TOCP significantly alters the general responsiveness to depolarization, and also affected neuritic structures. Thus, this reduction in general responsiveness to depolarization might be related to the reduced neurite area and the subsequent reduction in neurites equipped with voltage-gated calcium channels.

To identify a possible cause for the reduced glutamate sensitivity, we investigated the expression of NMDA and AMPA receptor subunits using qRT-PCR. The expression levels of both glutamate receptor subunits were significantly reduced on DIV 2 after 10 μM TOCP treatment. On DIV 7, though not significant, expression of the glutamate receptor also decreased. Therefore, 10 μM TOCP appears to inhibit receptor expression, which may be a possible mechanism explaining the reduced glutamate sensitivity. However, the results of the RNA expression data of the NMDA and AMPA receptor subunit genes cannot explain the reduced sensitivity of pCNs treated with 100 nM TOCP, and more research is needed to shed light on the underlying mechanisms of reduced glutamate signaling.

Increased intracellular calcium concentrations could represent a mode of action of TOCP neurotoxicity (El-Fawal and Ehrich, 1993; Wu *et al.*, 2003). Our estimate of the intracellular calcium concentration was based on the fluorescence ratio ΔR (f_{340}/f_{380}), with the data showing a significant increase in basal calcium after treatment with 10 μM TOCP, but not with lower concentrations. The elevated intracellular calcium levels observed with 10 μM TOCP may also cause cytotoxicity, neurite outgrowth inhibition and axon swelling via different Ca^{2+}-related intracellular mechanisms (e.g., calpain- or CaMK II-related pathways) (Leist and Nicotera, 1998). Furthermore, the elevated intracellular calcium levels may have contributed to the reduction of overall neuronal responsiveness by depolarization-dependent inactivation of voltage-gated ion channels.

Recently, TCPs including TOCP and its metabolites CBDP, have been discussed as causative agents of AS (Liyasova *et al.*, 2011). Symptoms of AS encompass the acute impairment of central nervous processes that are supposed to be caused by mechanisms different from those related to OPIDN. In the present *in vitro* study, we show neurotoxic effects of TOCP on glutamate-related signaling in central nervous system neurons. Our experimental setup is hardly comparable with the *in vivo* situation (e.g., lacking metabolism of TOCP). However, perturbed postsynaptic signaling, as indicated by our *in vitro* experiments, might be associated with neurobehavioral symptoms like difficulties with concentration/attention observed in AS. *In vivo*, the TOCP metabolite, CBDP was described as more toxic than TOCP itself, and therefore may be of greater relevance for AS. Due to binding studies with esterases, the toxicity of other TCP isomers is suspected to be much lower than TOCP neurotoxicity. Accordingly, commercial TCP mixtures used in aircrafts contain only a small amount of TOCP. Therefore, a next step for future *in vitro* studies should be (1) the investigation of CBDP and the other TCP isomers and their effect on glutamate-related responses in neurons, and (2) a closer look at the molecular mechanisms causing the decreased glutamate responsiveness.

In vivo studies showed that mice were susceptible to TOCP-induced delayed neuropathy (Lapadula *et al.*, 1985). Low TOCP concentrations were found in the spinal cords and brains of mice after 1 and 24 h TOCP treatment (Ahmed *et al.*, 1993, and Zhao *et al.*, 2006), showed that the cerebral cortex was more susceptible to TOCP-induced neurotoxicity than the spinal cord. Based on these *in vivo* data and the results shown by the present study, we suggest that (1) mouse pCNs, as used in our experiments, represent an adequate model to achieve a better understanding of TOCP effects on the central nervous system, and (2) functional endpoints are more sensitive than readouts focusing on neuronal structures.

In summary, our study shows that TOCP affects central nervous system neurons *in vitro* in a manner which may be relevant for symptoms of AS. As the most sensitive endpoint of TOCP-induced neurotoxicity, we identified effects on glutamate signaling. More specifically, the glutamate sensitivity of neurons was impaired at TOCP concentrations as low as 1 nM, and an effect on neurite morphology was observed at a higher concentration that still did not impact cell viability.

SUPPLEMENTARY DATA

Supplementary data are available online at http://toxsci.oxfordjournals.org/.

ACKNOWLEDGMENT

The authors are grateful to Christian Tigmann for his support in analyzing IMARIS data and Rosemarie Marchan for proofreading.

FUNDING

Bundesministerium für Bildung und Forschung (BMBF 0101-31P6541).

REFERENCES

Abou-Donia, M. B. (1993). The cytoskeleton as a target for organophosphorus ester-induced delayed neurotoxicity

(OPIDN). *Chemico-Biol. Interactions* **87**, 383–393.
Abou-Donia, M. B., Lapadula, D. M. and Suwita, E. (1988). Cytoskeletal proteins as targets for organophosphorus compound and aliphatic hexacarbon-induced neurotoxicity. *Toxicology* **49**, 469–477.
ACGIH. (2013) *TLVs® and BEIs®*. Signature Publications, Cincinnat.
Ahmed, A. E., Jacob, S., Soliman, S., Ahmed, N., Osman, K., Loh, J.-P. and Romero, N. (1993). Whole-body autoradiographic disposition, elimination and placental transport of [14C]Tri-o-cresyl phosphate in mice. *J. Appl. Toxicol.* **13**, 259–267.
Bowen, S. E., Batis, J. C., Paez-Martinez, N. and Cruz, S. L. (2006). The last decade of solvent research in animal models of abuse: Mechanistic and behavioral studies. *Neurotoxicol. Teratol.* **28**, 636–647.
Bushnell, P. J., Kavlock, R. J., Crofton, K. M., Weiss, B. and Rice, D. C. (2010). Behavioral toxicology in the 21st century: Challenges and opportunities for behavioral scientists. Summary of a symposium presented at the annual meeting of the neurobehavioral teratology society, June, 2009. *Neurotoxicol. Teratol.* **32**, 313–328.
Cao, Z., Shafer, T. J., Crofton, K. M., Gennings, C. and Murray, T. F. (2011). Additivity of pyrethroid actions on sodium influx in cerebrocortical neurons in primary culture. *Environ. Health Persp.* **119**, 1239–1246.
Chang, P.-A. and Wu, Y.-J. (2006). Effect of tri-o-cresyl phosphate on cytoskeleton in human neuroblastoma SK-N-SH cell. *Mol. Cell. Biochem.* **290**, 145–151.
Chen, J.-X., Sun, Y.-J., Wang, P., Long, D.-X., Li, W., Li, L. and Wu, Y.-J. (2013). Induction of autophagy by TOCP in differentiated human neuroblastoma cells lead to degradation of cytoskeletal components and inhibition of neurite outgrowth. *Toxicology* **310**, 92–97.
Danbolt, N. C. (2001). Glutamate uptake. *Prog. Neurobiol.* **65**, 1–105.
Dinh, N.-D., Chiang, Y.-Y, Hardelauf, H., Baumann, J., Jackson, E., Waide, S., Sisnaiske, J., Friamt, J. P., van Thriel, C., Janasek, D., *et al.*, (2013). Microfluidic construction of minimalistic neuronal co-cultures. *Lab Chip.* **13**, 1402–1412.
El-Fawal, H. A. N. and Ehrich, M. F. (1993). Calpain activity in organophosphorus-induced delayed neuropathy (OPIDN): Effects of a phenylalkylamine calcium channel blocker. *Ann. N. Y. Acad. Sci.* **679**, 325–329.
Emerick, G. L., Peccinini, R. G. and de Oliveira, G. H. (2010). Organophosphorus-induced delayed neuropathy: A simple and efficient therapeutic strategy. *Toxicol. Lett.*, **192**, 238–244.
Eto, M., Casida, J. E. and Eto, T. (1962). Hydroxylation and cyclization reactions involved in the metabolism of tri-o-cresyl phosphate. *Biochem. Pharmacol.* **11**, 337–352.
Flaskos, J. (2012). The developmental neurotoxicity of organophosphorus insecticides: A direct role for the oxon metabolites. *Toxicol. Lett.* **209**, 86–93.
Flaskos, J., McLean, W. G., Fowler, M. J. and Hargreaves, A. J. (1998). Tricresyl phosphate inhibits the formation of axon-like processes and disrupts neurofilaments in cultured mouse N2a and rat PC12 cells. *Neurosci. Lett.* **242**, 101–104.
Frimat, J. P., Sisnaiske, J., Subbiah, S., Menne, H., Godoy, P., Lampen, P., Leist, M., Franzke, J. and Hengstler, J. G. (2010). The network formation assay: A spatially standardized neurite outgrowth analytical display for neurotoxicity screening. *Lab Chip.* **10**, 701–709.
Gant, D. B., Eldefrawi, M. E. and Eldefrawi, A. T. (1987). Action of organophosphates on GABAA receptor and voltage-dependent chloride channels. *Fund. Appl. Toxicol.* **9**, 698–704.
Harrill, J. A., Freudenrich, T. M., Robinette, B. L. and Mundy, W. R. (2011). Comparative sensitivity of human and rat neural cultures to chemical-induced inhibition of neurite outgrowth. *Toxicol. Appl. Pharmacol.* **256**, 268–280.
Henschler, D. (1958). Die Trikresylphosphatevergiftung. Experimentelle Klärung von Problemen der Ätiologie und Pathogenese. *Klin. Wochenschr.* **36**, 663–674.
Kempermann, G., van Praag, H. and Gage, F. H. (2000). Activity-dependent regulation of neuronal plasticity and self repair. *Prog. Brain Res.* **127**, 35–48.
Krug, A., Balmer, N., Matt, F., Schönenberger, F., Merhof, D. and Leist, M. (2013). Evaluation of a human neurite growth assay as specific screen for developmental neurotoxicants. *Arch Toxicol.* **87**, 2215–2231.
Johnson, P. S. and Michaelis, E. K. (1992). Characterization of organophosphate interactions at N-methyl-D-aspartate receptors in brain synaptic membranes. *Mol. Pharmacol.* **41**, 750–756.
Lapadula, D. M., Patton, S. E., Campbell, G. A. and Abou-Donia, M. B. (1985). Characterization of delayed neurotoxicity in the mouse following chronic oral administration of tri-o-cresyl phosphate. *Toxicol. Appl. Pharmacol.* **79**, 83–90.
Leist, M. and Nicotera, P. (1998). Calcium and neuronal death. *Rev. Physiol. Biochem. Pharmacol.* **132**, 79–125.
Liyasova, M., Li, B., Schopfer, L. M., Nachon, F., Masson, P., Furlong, C. E. and Lockridge, O. (2011). Exposure to tri-o-cresyl phosphate detected in jet airplane passengers. *Toxicol. Appl. Pharmacol.* **256**, 337–347.
Pung, T., Klein, B., Blodgett, D., Jortner, B. and Ehrich, M. (2006). Examination of concurrent exposure to repeated stress and chlorpyrifos on cholinergic, glutamatergic, and monoamine neurotransmitter systems in rat forebrain regions. *Int. J. Toxicol.* **25**, 65–80.
Schmittgen, T. D. and Livak, K. J. (2008). Analyzing real-time PCR data by the comparative CT method. *Nat. Protoc.* **3**, 1101–1108.
Schöbel, N., Radtke, D., Lübbert, M., Gisselmann, G., Lehmann, R. and Cichy, A. (2012). Trigeminal ganglion neurons of mice show intracellular chloride accumulation and chloride-dependent amplification of capsaicin-induced responses. *PLoS ONE* **7**, e48005.
Slotkin, T. A., Seidler, F. J., Ryde, I. T. and Yanai, J. (2008). Developmental neurotoxic effects of chlorpyrifos on acetylcholine and serotonin pathways in an avian model. *Neurotoxicol. Teratol.* **30**, 433–439.
Song, F., Yan, Y., Zhao, X. and Zhang, C., (2009). Xie, K. Neurofilaments degradation as an early molecular event in tri-ortho-cresyl phosphate (TOCP) induced delayed neuropathy. *Toxicology* **258**, 94–100.
Song, F., Zou, C., Han, X., Zeng, T., Zhang, C. and Xie, K. (2012). Reduction of retrograde axonal transport associated-proteins motor proteins, dynein and dynactin in the spinal cord and cerebral cortex of hens by tri-ortho-cresyl phosphate (TOCP). *Neurochem. Int.* **60**, 99–104.
Stiegler, N. V., Krug, A. K., Matt, F. and Leist, M. (2011). Assessment of chemical-induced impairment of human neurite outgrowth by multiparametric live cell imaging in high-density cultures. *Toxicol. Sci.* **121**, 73–87.
van Thriel, C., Westerink, R. H., Beste, C., Bale, A. S., Lein, P. J. and Leist, M. (2012). Translating neurobehavioural endpoints of developmental neurotoxicity tests into in vitro assays and readouts. *Neurotoxicology* **33**, 911–924.
Wu, Y.-J., Chang, P.-A., Li, M., Li, Y.-X. and Li, W. (2003). Effect of tri-o-cresyl phosphate and methamidophos on 45Ca uptake by brain synaptosomes in hens. *Pestic. Biochem. Physiol.* **77**,

18–23.
Zhao, X.-l., Zhang, T.-l., Zhang, C.-l., Han, X.-y., Yu, S.-f. and Li, S.-X. (2006). Expression changes of neurofilament subunits in the central nervous system of hens treated with tri-ortho-cresyl phosphate (TOCP). *Toxicology* **223**, 127–135.